

RAPAKIVI GRANITES WITHIN PHANEROZOIC COLLISIONAL OROGENS AS A POSSIBLE CONSEQUENCE OF CONTINENTAL SUBDUCTION AND FOLLOWING EXHUMATION OF THE PRECAMBRIAN CRUST: EVIDENCES FROM THE PERMIAN JANGART RAPAKIVI IN SOUTH TIEN SHAN COLLISIONAL BELT, EASTERN KYRGYZSTAN

Leonid I. Solomovich, Boris A. Trifonov, USA, Russia

***Annotation:** The article discusses Rapakivi granites formed during the collision of tectonic plates that led to the formation of Phanerozoic mountains. In particular, the Permian granites of Jangart Rapakivi around the southern Tien Shan are considered. Since these stones are among the most ancient, the Earth will be a direct evidence of understanding the geological evolution of our city.*

***Key word:** granite, phanerozoic collision orogeny, tectonic plates*

РАПАКИВСКИЕ ГРАНИТЫ В ПРЕДЕЛАХ ФАНЕРОЗОЙСКИХ КОЛЛИЗИОННЫХ ОРОГЕНОВ КАК ВОЗМОЖНОЕ СЛЕДСТВИЕ КОНТИНЕНТАЛЬНОЙ СУБДУКЦИИ И ПОСЛЕДУЮЩЕЙ ЭКСГУМАЦИИ ДОКЕМБРИЙСКОЙ КОРЫ: СВИДЕТЕЛЬСТВА ПЕРМСКОГО ДЖАНГАРТА РАПАКИВИ В ЮЖНО-ТЯНЬ-ШАНЬСКОМ КОЛЛИЗИОННОМ ПОЯСЕ, ВОСТОЧНЫЙ КЫРГЫЗСТАН

Л.И. Соломович, Б.А. Трифонов, США, Россия, eakr.info@gmail.com

***Аннотация:** В статье обсуждаются граниты Рапакиви, образовавшиеся во время столкновения тектонических плит, которые привели к образованию фанерозойских гор. В частности, рассматриваются пермские граниты Джангарт Рапакиви вокруг Южного Тянь-Шаня. Поскольку эти камни являются одними из самых древних, Земля станет прямым свидетельством понимания геологической эволюции нашего города.*

***Ключевые слова:** гранит, фанерозойские коллизионные орогены, тектонические плиты*

1. Introduction

Rapakivi granites of the Proterozoic age occur on all continents (Fig. 1) and presumably represent the most voluminous silicic magmatism on the Earth (Ramo and Haapala, 1995). They have been emplaced in an extensional tectonic setting not directly related to lithosphere convergence (Anderson and Bender, 1989). Geochemically and otherwise they are considered to be classical representatives of A2-type granites by Eby (1992). Proterozoic rapakivis form a truly bimodal association together with large volumes of contemporaneous basic rocks comprising mostly of anorthosite and gabbro. According to widely accepted magmatic underplating model anorthosites and other basic rocks are considered to be derivatives of upwelled mantle melts that introduced the heat and caused the anatexis of granulitic lower crustal domains (Christiansen et al., 1983; Haapala et al., 2005; Heinonen et al., 2010). In this classical scenario, well known similarity of the chemical composition of rapakivi with such typical granulite facies rocks as charnokites and enderbites (Collins et al., 1982) is evidence of an extensive melting of granulitic source, which was possible owing to high geothermal gradients within the Proterozoic crust and mantle (e.g. Hand et al., 1999). Thus, the outburst of rapakivi granite magmatism in middle Proterozoic and its following degradation toward Proterozoic termination were probably controlled by general cooling of the Earth (Larin, 2009).

However, rare examples of late-postcollisional rapakivis within Phanerozoic collisional orogens are also known (Fig. 1). They include: Paleozoic rapakivi of the Jangart complex in the South Tien Shan, Kyrgyzstan (Solomovich and Trifonov, 1991; Solomovich and Trifonov, 2002; Konopelko et al., 2007), Tatalin pluton in the Qaidam Basin, China (Lu et al., 2007), Coastal Main plutons, USA (Stewart, 1998); the Mesozoic rapakivi of Shahevan pluton in the Qinling orogen, China (Wang et al., 2002; Zhang et al., 2009a); Cenozoic rapakivi of the Basin and Range Province: the Spirit Mountain pluton, Nevada, (Haapala et al., 2005; Walker, 2006) and Kingston Peak, Little Chief and Shoshone plutons in the Death Valley, California, USA (Calzia and Ramo, 2005). In spite of remarkable petrological and geochemical similarity with their Proterozoic counterparts, Phanerozoic rapakivi magmatic association usually lack anorthosite or any signifi-

cant volume of other contemporaneous basic rocks. Thus, the applicability of mantle melt underplating hypothesis to explain their origin is highly questionable. On the other hand, all known occurrences of Phanerozoic A-type granites with typical rapakivi texture were found within those collisional orogens where ultra-high pressure (UHP) coesite bearing metamorphic rocks of a close age were also found (Fig. 1), suggesting a connection of their petrogenesis with a deep continental subduction (Solomovich, 2007). But UHP metamorphic terranes are much more common than Phanerozoic rapakivis. More than forty UHP terranes within more than twenty orogenic belts have been documented around the world (Liou et al., 2009; Zhang, 2011). One more constrain for the Phanerozoic rapakivi appearance is that they occur in only those collisional orogens where the Precambrian craton crust was overridden by orogenic complex (Fig. 1).

The Jangart rapakivi complex of the Early Permian age, occurring in the Late Paleozoic South Tien Shan collisional belt (STCB), is considered to be a key subject for the development of an alternative petrogenetic model for the Phanerozoic rapakivis, which links the formation of these rocks to the processes of deep subduction and subsequent exhumation of ancient continental crust.

Being a constituent of late-postcollisional magmatism within STCB, the Jangart rapakivis may also somehow relate to the huge Permian magmatic domain or large igneous province (LIP) overlapping the North Tarim and Chinese and Kyrgyz Tien Shan and consisting of wide range of basic, alkaline and acid rocks. The origin of this domain remains controversial, but many researchers attribute it to the mantle plume activity (e.g. Yang et al., 2007; Pirajno et al., 2008; Zhang et al., 2010a,b; Qin et al., 2011). In this article we summaries all published and unpublished new data concerning the Jangart rapakivis in the context of their geological setting within both STCB and LIP. Then we will discuss the suggested petrological model.

2. Regional geological setting

The Jangart rapakivi granite complex occurs within the Late Paleozoic South Tien Shan collisional belt (STCB), which is the most southern part of the giant Central Asian orogenic belt. It is generally accepted that STCB resulted from closure of the Turkestan Ocean followed by oblique collision between the Tarim Precambrian craton and the Caledonian Kazakhstan-Yili (Kazakh) continent (Biske, 1996; Chen et al., 1999) (Fig. 2). The Kyrgyz portion of STCB, which is about 1100 km in length, consists of two segments divided by the largest in the Central Asia the Talas-Fergana diagonal dextral strike-slip fault (TFF). Those segments remarkably differ from each other by the thickness of continental crust, type of regional metamorphism and late-postcollisional magmatism (Solomovich, 2007). The relatively wide Alay segment situated to the west of TFF is characterized by moderately thickened (45- 55 km) crust (Sabitova, 1989) and high temperature/low pressure zoned regional metamorphism (Bakirov, 1978) containing relics of granulite facies rocks Nenakhov et al., 1992).

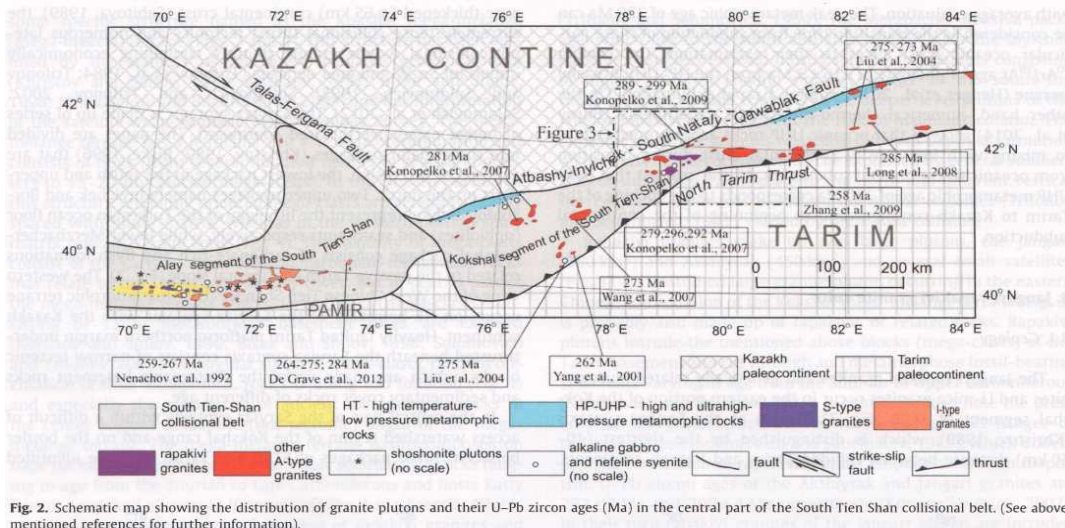


Fig. 2. Schematic map showing the distribution of granite plutons and their U-Pb zircon ages (Ma) in the central part of the South Tien Shan collisional belt. (See above-mentioned references for further information).

The Permian magmatism in the Alay segment (Fig. 2) is represented by strongly peraluminous S-type granites, locally rooted in high-temperature/ low pressure metamorphic rocks, numerous calc-alkaline I-type granite plutons and small shallow level shoshonitic/ultrapotassic intrusions, that temporally alternate reciprocally with I-type granites.

Situated to the east of TFF the relatively narrow Kokshal segment is distinguished by over thickened (60-65 km) crust and occurrences of high to ultra- high-pressure (HP-UHP) metamorphic terranes. The eastern continuation of the Kokshal segment in the Chinese portion of STCB consists of the same top-to-the south nape structures as in the Kyrgyz portion. The Atbashi-West Chinese Tien Shan HP-UHP metamorphic belt extends for about 1300 km along the closing suture of the Turkestan Ocean. This belt consisting mostly of coesite bearing eclogites, pelitic, felsic and calcareous schists is considered to be only known HP-UHP belt in the world with mostly

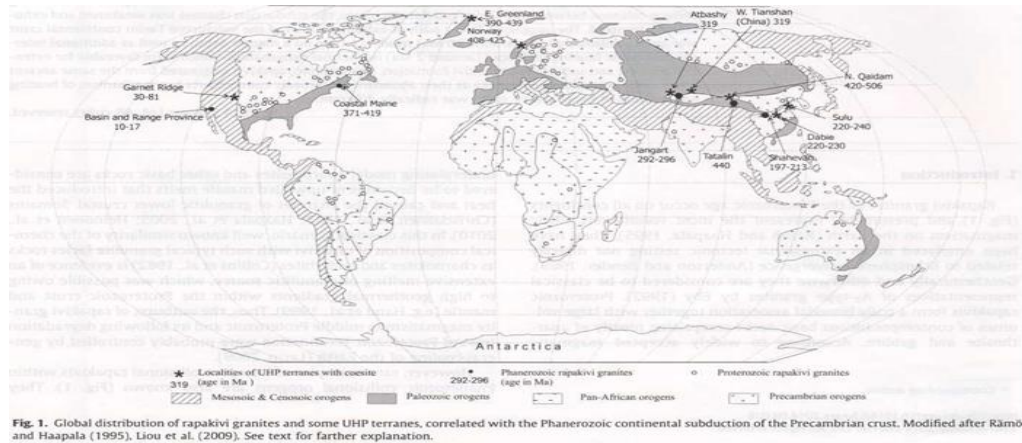


Fig. 1. Global distribution of rapakivi granites and some UHP terranes, correlated with the Phanerozoic continental subduction of the Precambrian crust. Modified after Råmo and Haapala (1995), Liou et al. (2009). See text for farther explanation.

oceanic crust protolith (Zhang, 2011). In contrast to the Alay segment, the Permian late-postcollisional magmatism within STCB to the east of TFF is represented almost exceptionally by A-type granites, including the Jangart rapakivi (Fig. 2). That distinction of STCB segments is believed to be evoked by the difference in style of continental collision in each segment (Solomovich, 2007). In particular, to the east of TFF the collision was followed by the continental subduction of the Tarim beneath STCB. The Tarim continental subduction was initially inferred on the basis of geological (Biske, 1996; Chen et al., 1999), petrological and Nd-isotopic arguments. The Late Paleozoic underthrusting of the Tarim beneath STCB at a distance of 50-100 km was later defined by the seismic profiling in western part of the Kokshal segment of STCB.

The time estimation of collision between the Tarim craton and Kazakh continent are contradictory and vary from Late Devonian- Early Carboniferous to Late Permian-Triassic (see Han et al., 2011 for detailed bibliography). The main reason for this contradiction is probably that the closing of the Turkestan Ocean occurred in scissors-like manner from east to west (Chen et al., 1999). However, for greater central portion of STCB shown in Fig. 2 most researchers place collision into more narrow time span between Early Carboniferous and Early Permian. The lower-age bound for the beginning of collision is provided by the youngest radiolarians and conodonts of the Early Carboniferous age found within ophiolitic melange. The youngest paleontological ages of the Turkestan Ocean deep-water sediments not related to ophiolitic melange are also the Early Carboniferous (Biske et al., 2012). The lower-age bound for collision termination was established by the presence of the Latest Carboniferous to Permian molassa, which unconformably overlays HP-UHP eclogites and contains their gravels. The upper age limit for collision termination is probably provided by the emplacement of the Early Permian rapakivi granites, which are the eldest stitching granites in STCB with U-Pb zircon age of 299-292. But it is important to note that the southward movement of napes continued at least locally in the Early Permian, suggesting late-collisional emplacement of rapakivi.

The numerous isotope dating of HP-UHP eclogites are generally compatible with geological data. In the Kyrgyz portion of STCB (Atbashi terrane) peak metamorphic ages of

subducted materials was estimated as 324-327 Ma by $^{40}\text{Ar}/^{39}\text{Ar}$ dating and 319 ± 4 Ma by Sm/Nd isochrone. In the Chinese South Tien Shan peak metamorphic ages for eclogites were established as following; 308.9 ± 2 to 326 ± 5.2 Ma by Lu-Hf and Sm-Nd isochrone, 319.5 ± 2.9 Ma and 318 ± 3.3 Ma by U-Pb zircon (Su et al., 2010) and 313-316 Ma by Lu-Hf isochrone. SHRIMP U-Pb zircon dating of coesite-bearing metapelite yielded the peak metamorphic age 320.4 ± 3.7 Ma, which is in range with eclogites. The consistent results from independent geochronological techniques clearly demonstrate that all UHP rocks with oceanic crust protolith formed on the boundary between Lower and Upper Carboniferous in average about 320 Ma ago. It is important to note that U-Pb zircon ages, which are less susceptible to isotope reequilibration during exhumation and provide more accurate dating of UHP metamorphic events (Zheng, 2012), for both eclogites and metapelites are similar and coincide with average evaluation. The peak metamorphic age of 320 Ma can be considered as the transition time from subduction of those particular oceanic crust slices to their exhumation. The cooling $^{40}\text{Ar}/^{39}\text{Ar}$ age of phengite of 316 ± 3 Ma from the HP-UHP Atbashy terrane (Henger et al., 2010) implies a rapid exhumation. On the other hand,

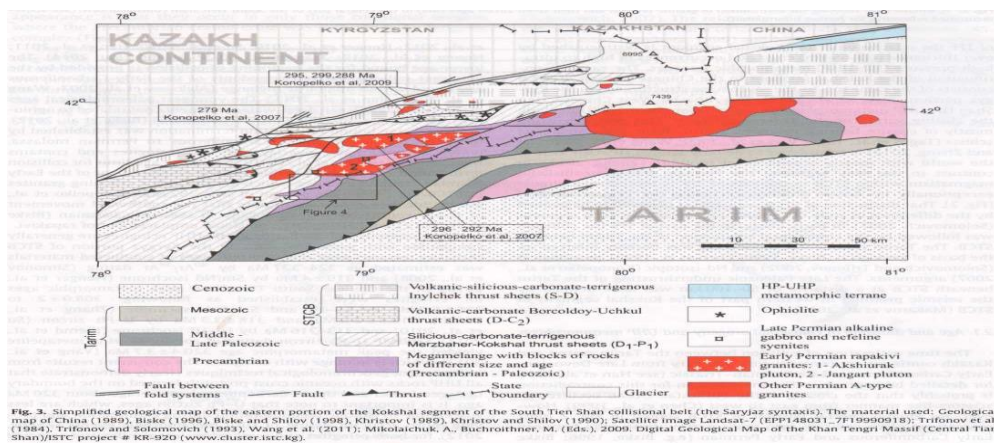


Fig. 3. Simplified geological map of the eastern portion of the Kokshal segment of the South Tien Shan collisional belt (the Saryjaz syntaxis). The material used: Geological map of China (1989), Biske (1996), Biske and Shilov (1998), Khrstov (1989), Khrstov and Shilov (1990); Satellite image Landsat-7 (EPP148031_7F0990018); Trifonov et al. (1988), Trifonov and Solomovich (1993), Wang et al. (2011); Mikolajchuk, A., Buchrothner, M. (Eds.), 2009. Digital Geological Map of the Khan Tengri Massif (Central Tianshan)/ISGC project # RR-920 (www.cluster.isgc.kg).

numerical thermo-mechanical experiments (Burov et al., 2014) showed that oceanic UHP rocks are exhumed thanks to mixing with low-density continental crust during transition from oceanic to continental subduction. All this suggest that peak UHP metamorphic age of 320 Ma corresponds to the docking of the Tarim to Kazakh continent and to beginning of the continental subduction.

3. Jangart rapakivi granite suite

3.1. Geology

The Jangart rapakivi granites and genetically related leucogranites and Li-mica granites occur in the eastern portion of the Kokshal segment of STCB (Fig. 3), known as the Saryjaz syntaxis, which is distinguished by the shortest (40- 50 km) distance between collided Tarim and Kazakh continents, over thickened (~ 65 km) continental crust, the extremely tense collisional thrust tectonics and numerous late-postcollisional A-type granite plutons, containing economically important Sn-W and gold deposits. The Saryjaz syntaxis is made up of series of folded napes overthrust southward. The napes are divided into three major packages that are exposed in succession, the lowest package in the south and uppermost on the north. Two upper packages namely Inylchek and Bor-koldoy-Uchkul represent the lithology of the Turkestan ocean floor (ophiolites) and seamounts respectively, while lower Merzbacher-Kokshal package consists of carbonate-rich and flysch formations related to the passive Tarim continental slope (Fig. 3). The western wing of the West Chinese Tien Shan HP-UHP metamorphic terrane occurs on NE boundary of the Saryjaz syntaxis with the Kazakh continent. Heavily faulted Tarim platform northern margin under-thrust beneath the Saryjaz syntaxis consists of narrow tectonic blocks, which are made up of the Proterozoic basement rocks and sedimentary cover rocks of different age.

In the central part of the Saryjaz syntaxis within a difficult of access watershed region of the Kokshal range and on the border between thrust packages of STCB and Tarim we have identified some specific structure named as the Kokshal mega-melange (mega-breccia) terrane

(Figs. 3 and 4). This structure has been outlined by the analysis of the latest available geological data and our interpretation of the satellite imagery made by US Geology Survey. The megamelange terrane has a lenticular (20 x 120 km) configuration and consists of huge (from several hundred meters to several kilometers to 15-20 km) blocks (mega-clasts). In the eastern portion of this structure randomly oriented mega-clasts are generally closely spaced with minor matrix, whereas in the western portion shaly matrix prevails significantly (Fig. 4). The majority of mega-clasts consist of the Early to Late Paleozoic carbonate-terrigenous rocks that relate to the Tarim sedimentary cover. But in central part of the mega-melange terrane (Fig. 3) large blocks (mega-clasts) consisting of Tarim metamorphic basement rocks are exposed. An angular shape of mega-clasts, random orientation of their elongations, rock's bedding and foliation (Fig. 4) and especially the occurrence of ancient metamorphic rocks in the center suggest a diapiric (not tectonic) origin of the megamelange terrane. The mega-melange terrane is superimposed on nape packages and cuts through Paleozoic sedimentary rocks ranging in age from the Silurian to Late Carboniferous and hosts Early Permian rapakivi plutons as if cementing the mega-breccia. All this suggests almost synchronous formation of rapakivi granites and mega-melange terrane and their possible genetic relation. There is some vertical and lateral zoning in the spatial distribution of genetically related A-type granites in the Saryjaz syntaxis. This zoning generally reflects different level of erosion of presumably single magmatic column within distinct tectonic units of the Saryjaz syntaxis. The northern an upper most Inylchek thrust package hosts shallow-level small stocks of highly differentiated rare metal leucogranites and Li-mica granites (Fig. 3). The dyke suite of those granites is represented by Li-F felsite porphyry (ongonite) and K-B porphyry (elvane). The Merzbacher-Kokshal package, which lies to the south and structurally under the Inylchek package hosts less evolved mostly middle size plutons consisting of biotite granites. Finally, situated farther to the south the mega-melange terrane contains large, deeper level plutons of the Jangart rapakivi that represent the root of magmatic column. The exposure of A-type granites related to different depth of formation on the current level of erosion can be explained by general submersion of subducted Tarim plate to the north and different vertical movement of individual blocks during Alpine tectonics, caused by India-Asia collision.

Rapakivi granites make up two large plutons, the Jangart (350 km²) and Akshiyarak (450 km²) and several small satellites (Fig. 3). An unstudied large granite pluton occurring in the eastern Chinese continuation of the Kokshal mega-melange terrane (Fig. 3) is probably also made up of rapakivis or related rocks. Rapakivi plutons intrude the mentioned above blocks (mega-clasts) It is important to note the presence of the protoclastic texture within endocontact fringes of rapakivi plutons, which underline the connection of rapakivi plutons emplacement with diapirism. U-Pb zircon ages of the Akshiyarak and Jangart granites are 292 ± 3 Ma and 296 ± 4 Ma respectively. In their turn rapakivi granites of the

Jangart pluton are intruded by small stocks consisting of alkaline gabbro, nepheline syenite and carbonatite (Solomovich and Trifonov, 1991) (Fig. 3). The similar alkaline rocks with U-Pb zircon age of 274 ± 2 Ma are described on the North Tarim.

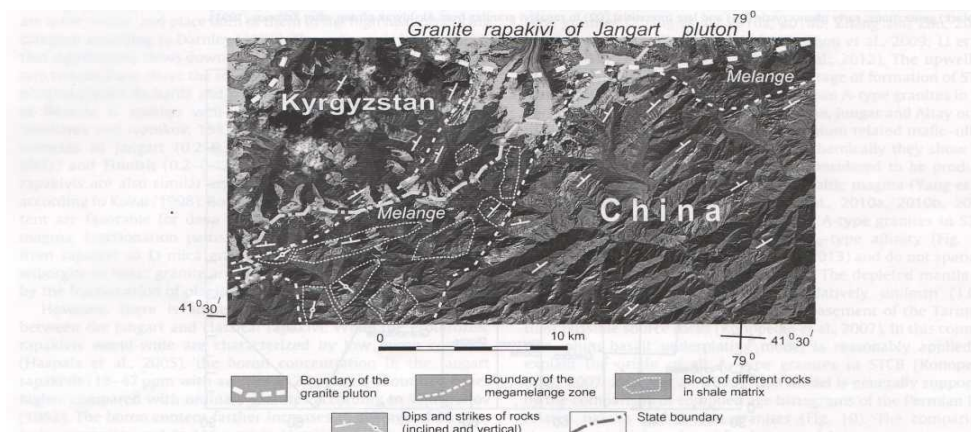


Fig. 4. A fragment of the southwestern part of the Kokshal mega-melange (mega-breccia) terrane according to interpretation of the satellite image Landsat-7 (EPP148031_7F1990918). Carbonate-terrigenous rocks of megaclasts in accordance with available data relate to the Devonian-Late Carboniferous. The satellite image has been downloaded via the USGS portal (<http://landsat.usgs.gov/>). See text for farther explanation.

3.2. Petrology and geochemistry

The detailed petrologic and geochemical description of the Jangart rapakivi as well as other A-type granites in the Saryjaz syntaxis can be found in some previous publications (Solomovich and Trifonov, 1991; Solomovich and Trifonov, 2002; Konopelko et al., 2007). In this paper we place special emphasis on the comparison of Jangart rapakivis with their classical Finnish counterparts and other A-type granites in STCB occurring beyond the Saryjaz syntaxis.

By outward appearance, petrographic texture and mineral composition Jangart rapakivi is quite similar to its classical analogue (Solomovich and Trifonov, 1991; Trifonov, 1991). Ovoidal rapakivi, varying in composition from granite to granosyenite, is coarsegrained, densely porphyritic and occasionally exhibit a trachytoid fabric. In typical varieties 30-40% of K-feldspar megacrysts are surrounded by oligoclase rims to create a rapakivi-textured mantle (Fig. 5a and b). The presence of two generations of quartz crystals (Fig. 5c) is also typical. Major minerals are perthitic microcline (40-60%), plagioclase (15-20%), quartz (15-30%), biotite (5-10%) and hornblende (2-7%). Accessory minerals include allanite, zircon, apatite, fluorite, titanite, ilmenite and magnetite. Iddingsite pseudomorphs at the expense of fayalite and small wustite globules

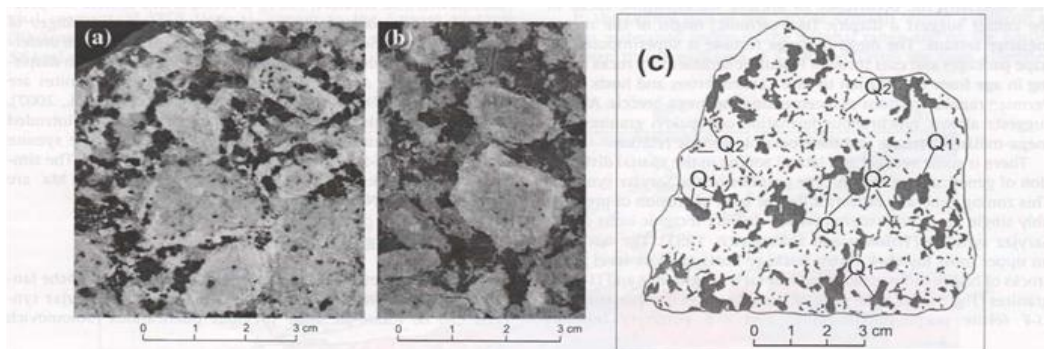


Fig. 5. Texture of Kokshal rapakivi granites. Ovoidal K-feldspar rapakivi granites from Jangart pluton (a and b), after Konopelko et al. (2007). Microdrawing (c) of two quartz (black) generations: early phenocrystic (Q1) and late interstitial (Q2) in rapakivi granites from Akshiyak pluton, after Trifonov (1991).

with native iron cores are found in some samples with low quartz content, suggesting the low oxygen fugacity and reduced character of parental magma, typical of all rapakivi granites (Shinkarev and Ivanikov, 1983). Unlike the rest of A-type granites in STCB, which are more leucocratic, Jangart rapakivis as well as Finnish ones fall within field of granosyenite in the TAS diagram (Fig. 6). But it is important to note that samples of Jangart and Finnish rapakivis with the equal $K_2O + Na_2O$ content differ from each other by K/Na ratio, which is slightly higher in Finnish rocks (1.8 vs. 1.6) (Solomovich and Trifonov, 1991). Both Jangart and Finnish rapakivis are metaluminous ($molar\ Al_2O_3 / (CaO + K_2O + Na_2O) < 1$) with high (0.85-0.95) molar $FeO_t / (FeO_t + MgO)$ ratio. The same ratio in biotite is especially high and close to 1 (Solomovich and Trifonov, 1991; Haapala et al., 2005).

In REE diagram (Fig. 7a) the Jangart rapakivis are nearly identical to their Finnish counterparts. The multi-element graphs (Fig. 7b) are also very similar with the exception that Finnish rocks, probably owing to higher K/Na ratio, have slightly more pronounced Rb-maximum and higher values of Zr and Hf. As well as Finnish rocks Jangart rapakivis exhibit strong geochemical characteristics of A-type granites, including high content of HFS elements, high Ga/Al, Rb/Ba and Rb/Sr values (Solomovich and Trifonov, 2002; Konopelko et al., 2007). Both of them also plot into A-type field of Whalen et al. (1987), A2-type field of Eby (1992) and within-plate granite field of Pearce et al. (1984) diagrams (Fig. 8a-c). Negative $sNd(t)$ values of Jangart rapakivis (-4.8 to -6.9) (Konopelko et al., 2007) are in range with those of the Fennoscandian Shield (0 to -9.0) (Haapala et al., 2005) suggesting crustal sources of the parental magma.

World-wide rapakivis are notable for their high content of radiogenic heat-producing elements such as K, U and Th. The concentrations of these elements in Jangart (U-in range of 3-9 ppm; Th-in range of 19-52 ppm) (Konopelko et al., 2007) and Finnish Wiborg (U-8 ppm; Th-25 ppm) (Haapala et al., 2005) rapakivis are quite similar and place both of them in the high heat producing category according to Darnley (1986). The radiogenic heat production significantly slows down rate of magma cooling and can maintain temperature above the solidus for up to 10-20 Ma within large plutons (Willis-Richards and Jackson, 1989). A high concentration of fluorine is another well-known peculiarity of rapakivi (e.g. Shinkarev and Ivanikov, 1983; Haapala et al., 2005). The fluorine contents in Jangart (0.2-0.35 wt.%) (Solomovich and Trifonov, 2002) and Finnish (0.2-0.42 wt.%) (Simonen and Vormaa, 1969) rapakivis are also similar and close to that of rare-metal granite according to Koval (1998). Both slow cooling and high fluorine content are

favorable for deep crystal fractionation of the parental magma. Fractionation paths of granites in the Saryjaz syntaxis from rapakivi to Li mica granite and the Finnish rapakivi from wiborgite to topaz granite are identical (Fig. 9) and caused mostly by the fractionation of plagioclase, K-feldspar and biotite.

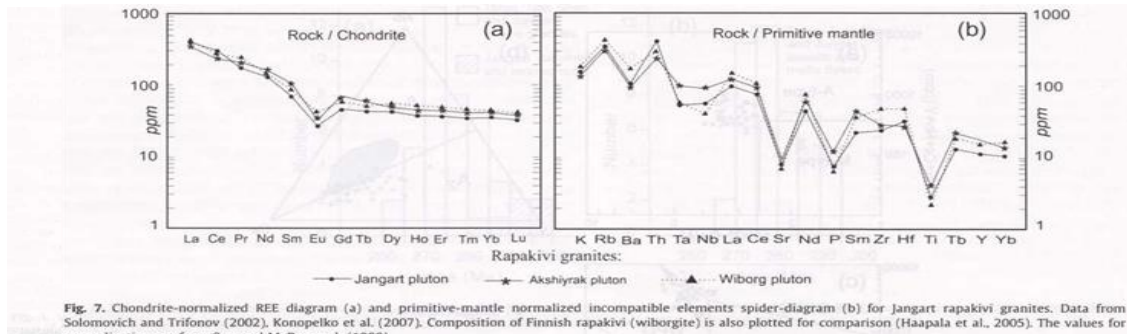


Fig. 7. Chondrite-normalized REE diagram (a) and primitive-mantle normalized incompatible elements spider-diagram (b) for Jangart rapakivi granites. Data from Solomovich and Trifonov (2002), Konopelko et al. (2007). Composition of Finnish rapakivi (wiborgite) is also plotted for comparison (Haapala et al., 2005). The values for normalization are from Sun and McDonough (1989).

However, there is some important geochemical difference between the Jangart and classical rapakivi. While the Proterozoic rapakivis world-wide are characterized by low boron contents (Haapala et al., 2005), the boron concentration in the Jangart rapakivis (18-47 ppm with average of 25 ppm) is about two times higher compared with ordinary granites according to Vinogradov (1962). The boron content farther increases to average of 50 ppm in leucogranites and to 115 ppm in Li-mica granites (Solomovich et al., 2012). The enrichment of A-type granites of the Saryjaz syntaxis in both fluorine and boron radically increases their potential for economic Sn and Sn-W mineralization. As main source of boron in granites is considered to be metasedimentary rocks (e.g. Trumbull et al., 2008), assimilation of the juvenile Late Paleozoic crust in late-postcollisional setting could have some influence upon the formation of the Saryjaz A-type granites. This assumption is collaborated by the strong variation of the initial $^{87}\text{Sr}/^{86}\text{Sr}$ ratio (Sr_0 from 0.7080 to 0.7256) within leucogranites, suggesting the heterogeneity of source rocks (Solomovich and Trifonov, 2002).

4. Discussion

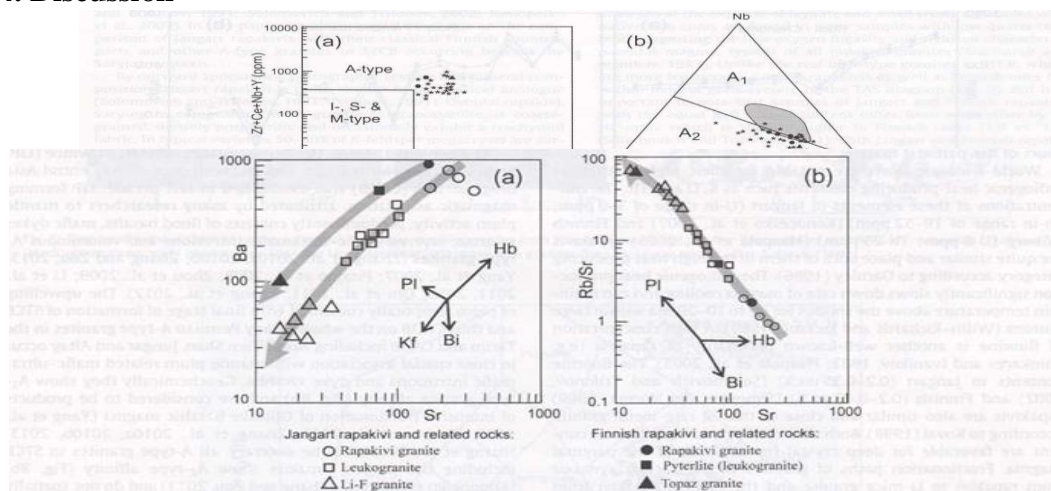


Fig. 9. Ba vs. Sr (a) and Rb/Sr vs. Sr diagrams showing crystal fractionation process of Jangart and Finnish rapakivi magmas. Partition coefficients are from Rollinson (1993). Symbols: Pl-plagioclase, Kf-K-feldspar, Hb-hornblende, Bi-biotite. Data from: Solomovich and Trifonov (2002), Konopelko et al. (2007), Haapala et al. (2005).

4.1. Possible mantle plume connection and basalt underplating

As mentioned above, the Permian large igneous province (LIP) embracing the North Tarim and southern part of the Central Asia orogenic belt (CAOB) was established in last decade. LIP forming magmatic association, attributed by many researchers to mantle plume activity, predominantly consists of flood basalts, mafic dykes swarms, layered mafic-ultramafic intrusions and voluminous A-type granites (Zhang et al., 2010a, 2010b; Zhang and Zou, 2013; Yang et al., 2007; Pirajno et al., 2008; Zhou et al., 2009; Li et al., 2011, 2012; Qin et al., 2011; Zhang et al., 2012).

The upwelling of plume temporally coincided with final stage of formation of STCB and thus CAOB on the whole. Many Permian A-type granites in the Tarim and CAOB including

including North Tien Shan, Jungar and Altay occur in close spatial association with mantle plum related mafic-ultramafic intrusions and dyke swarms. Geochemically they show Ar type granite affinity (Fig. 8b) and are considered to be products of intensive fractionation of OIB-like basaltic magma (Yang et al., 2007; Pirajno et al., 2008; Zhang et al., 2010a, 2010b, 2013; Huang et al., 2012). To the contrary, all A-type granites in STCB including the Jangart rapakivi show A2-type affinity (Fig. 8b) (Konopelko et al., 2007; Zhang and Zou, 2013) and do not spatially associate with mafic-ultramafic plutons. The depleted mantle Nd model ages of those granites are relatively uniform (1.05- 1.43 Ga) and point to the Precambrian basement of the Tarim as their possible source rocks (Konopelko et al., 2007). In this connection, plum basalt underplating model is reasonably applied to explain the origin of all A2-type granites in STCB (Konopelko et al., 2007; Zhang et al., 2013). This model is generally supported by the comparison of compiled age histograms of the Permian LIP- related basalts and A-type granites (Fig. 10). The comparison shows that initial, peak and final stages of A-type granitic magmatism postdate those particular stages of basalt magmatism for about 5 Ma correspondingly. This 5 Ma time span probably enough for basalt magma fractionation to produce A-type granites outside STCB or for heating and melting of the Tarim basement rocks to form A2-type granites inside STCB. But all this does not relate to the Jangart rapakivis, which started to emplace before the oldest basalts did (Fig. 10a). Rapakivis also lack any mafic microgranular enclaves and sinplutonic mafic dykes, which are common for the rest of A-type granites in the Kokshal segment of STCB beyond the Saryjaz syntaxis (Solomovich, 2007). Finally, as mentioned above, rapakivi were intruded by alkaline rocks (Solomovich and Trifonov, 1991) related to mantle plum activity (Zhang et al., 2008). Thus the basalt underplating hypothesis is not applicable to explain the Jangart rapakivi petrogenesis.

However, all mentioned above does not rule out a possibility of some positive dynamic influence of mantle plum upwelling upon the rapakivi formation. The arriving of mantle plum to the asthenosphere, which probably occurred some millions of years before rapakivi emplacement, could cause some decompression within the subduction channel, thus facilitating the previously subducted continental crust exhumation.

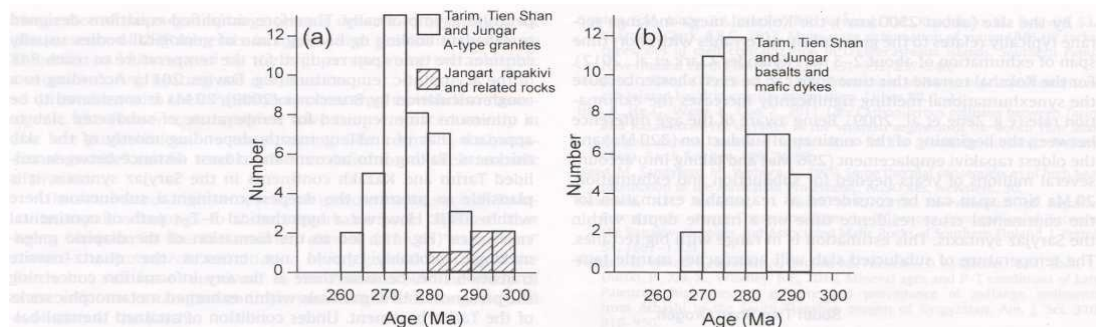


Fig. 10. Histograms of compiled U-Pb zircon age data: (a) Tarim, Tien Shan and Jungar A-type granites ($n = 42$); (b) Tarim, Tien Shan and Jungar basalts and mafic dykes ($n = 47$). Data sources: Konopelko et al. (2007, 2009), Long et al. (2008), Zhang et al. (2010a,b, 2012), Qin et al. (2011), Huang et al. (2012).

4.2. Continental subduction and exhumation connection

According to mentioned above seismic data (Makarov et al., 2010) the Tarim continental crust subducted beneath STCB at low angle was trapped within lithospheric mantle and never exhumed. A low initial subduction angle that creates too much friction along the upper subduction channel boundary for revers motion might be one of main reason that prevents continental crust exhumation (Brueckner, 2009). But on the other hand, while continental subduction resulting in the formation of UHP rocks usually takes place along the whole collisional belt, spatial distribution of UHP terranes around the world suggests that their exhumation occurs only locally in specific sites, characterized by geometrical or structural complexities (Boutelier and Chemenda, 2008) such as the obliquity of plate convergence, existence of strike-slip/transform fault, cutting oblique the interplate zone or the curvilinear geometry of the plate boundary. The Saryjaz syntaxis definitely possesses many of those features. Indeed, within the Saryjaz syntaxis the collisional suture separating STCB from the Kazakh continent is characterized by flexure-like bending complicated by NE left-lateral strike-slip tectonics (Fig. 3). For regional sinistral shearing tectonics caused by oblique collision between the Tarim and Kazakh continents (Bazhenov et al., 1999) it is quite typical the appearance of local extension environment in areas with similar flexure. The thermo-mechanical physical modeling of such kind of environment (Boutelier and Chemenda, 2008) showed a local reduction of the interplate pressure that permits

the rise of deeply subducted low-density continental crust under buoyancy force. Additionally, the latest thermo-mechanical numerical modeling (Burov et al., 2014) showed that UHP rocks exhumation on the crustal level (~ 40 km depth) is rapid and is driven by buoyancy of partly metamorphosed or partly molten UHP material often mixed with non-metamorphosed crustal volumes. In the context of all these geological and experimental data, the origin of the described above diapiric mega-melange (mega-breccia) terrane, which hosts the Jangart rapakivi, can be considered as the consequence of exhumation of deeply subducted Tarim continental crust slices.

4.3. Jangart rapakivi formation

Some traces of sinexhumation anatexis of HP-UHP rocks were noticed in many terranes (e.g. Lang and Gilotti, 2007; Gordon et al., 2012; Chen et al., 2013). But an extensive high degree melting of HP-UHP rocks is different and might be possible under some specific conditions, namely with long residence time of source rocks in a mantle depth allowing the subducted slab temperature to approach the temperature of surrounded mantle and with a rapid exhumation allowing isothermal decompression and subsequent melting of source rocks. Meanwhile, according to comparative analyses (Kylander-Clark et al., 2012) all well-studied worldwide HP-UHP terranes with few exception can be divided into two separate groups; large (tenth of thousands km²) terranes that evolved and exhumed slowly (over 10-30 Ma) and small ones (hundred and first thousands km²) that formed and were exhumed rapidly on time scale of <10 Ma. It is clear that each of those groups meets only one of the two mentioned above main conditions for extensive melting, which can explain its rarity.

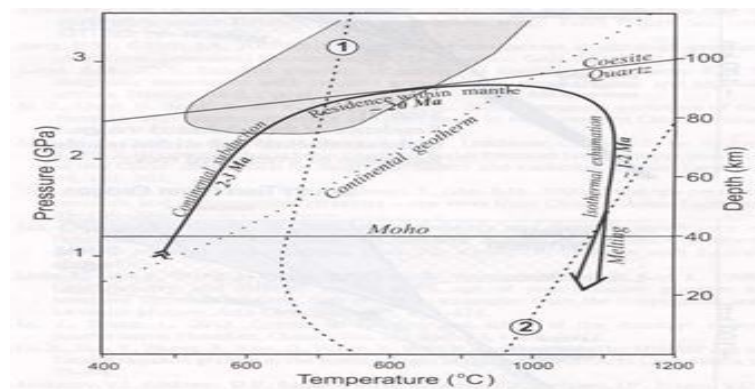


Fig. 11. Schematic diagram showing possible P-T-t path of the Tarim continental crust slices within the Saryjaz syntaxis, starting from continental subduction to exhumation and decompression melting. The shaded area represents the stability field of HP-UHP eclogite-facies terranes (Brueckner, 2009). Dashed lines are the wet (1) and dry (2) solidus for granite (Huang and Wyllie, 1973). The quartz-coesite transition is from Bohlen and Boettcher (1982).

By the size (about 2500 km²), the Kokshal mega-melange terrane typically relates to the group of small terranes with short time span of exhumation of about 2-3 Ma (Kylander-Clark et al., 2012). For the Kokshal terrane this time span can be even shorter because the synexhumational melting significantly increases the exhumation rate (e.g. Zeng et al., 2009). Being aware of the age difference between the beginning of the continental subduction (320 Ma) and the oldest rapakivi emplacement (296 Ma) and taking into account several millions of years needed for subduction and exhumation, 20 Ma time span can be considered as reasonable estimation for the continental crust residence time on a mantle depth within the Saryjaz syntaxis. This estimation is in range with big terranes. The temperature of subducted slab will approach mantle temperature asymptotically. Therefore simplified equations designed to calculate cooling or heating time of geological bodies usually consider the time span required for the temperature to reach 84% of the asymptotic temperature. According to a rough calculation by Brueckner (2009), 20 Ma is considered to be a minimum time required for temperature of subducted slab to approach that of ambient mantle depending mostly of the slab thickness. Taking into account the closest distance between collided Tarim and Kazakh continents in the Saryjaz syntaxis, it is plausible to presume the deepest continental subduction there within STCB. However a hypothetical P-T-t path of continental crust slice (Fig. 11), led to the formation of the diapiric mega-melange, probably should not crosscut the quartz-coesite transition line, because there is no any information concerning the presence of UHP minerals within exhumed metamorphic rocks of the Tarim basement.

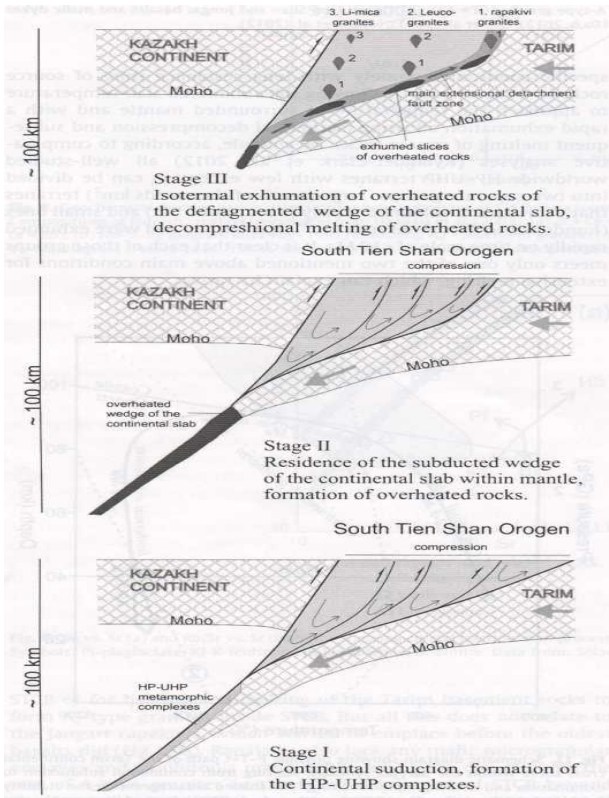


Fig. 12. Suggested formation model of the Jangart rapakivi and related A-type granites (leucogranite, Li-mica granite) in the Saryjaz syntaxis of STCB.

Under condition of attained thermal balance between the slab and ambient mantle the slab temperature depends only on depth and geothermal gradient. This temperature of about 950 °C, that corresponds to the depth of 90 km (Fig. 11) even being reduced to 84% of asymptotic temperature i.e. 800 °C is still higher than wet granite solidus. But it is not high enough to melt a dry refractory granulitic source rock of rapakivi even after adiabatic decompression (Fig. 11). However, additional heat will be generated by the radioactive decay of K, U and Th. The most of crustal radiogenic heat is usually released into atmosphere, but if the continental crust is trapped within mantle, the loss of radiogenic heat will be reduced or even eliminate, so as time passes the subducted slab will be hotter than ambient mantle (Brueckner, 2009). The average Precambrian crust radiogenic heat production is about 2.7 pW/m³ (Pinet and Jaupart, 1987). With the average rock density of 2700 kg/m³ and specific heat of about 1000 J/kg °C (Davies, 2011) it takes c. 30,000 years to raise the temperature of 1 kg of slab by 1 °C. Thus around 10 Ma are required to raise temperature by 300 °C. By a minimum scenario the attained temperature of about 1100 °C is sufficient for the deepest part of slab consisting of granulites to cross the dry granite solidus line below Moho under condition of isothermal decompression (Fig. 11).

The partially melted rocks become highly ductile and may move upward as a diapir (e.g. Whitney et al., 2004). Besides many researchers (e.g. Clifta et al., 2004; Cottle et al., 2007; Osozawa and Wakabayashi, 2012) suggest that the exhumation on the crustal level is driven by extensional detachment faulting. In this context the border between the consolidated collisional wedge of STCB and the subducted slab of the Tarim could act as the main extensional detachment fault zone (Fig. 12), channeling the exhumation of overheated continental crust slices. Higher degree of melting that occurred on the crustal level led to the separation of rapakivi magma with subsequent intrusion into mega-melange terrane. The crystal fractionation of the parental rapakivi magma within intermediate chambers led to formation of rare-metal leucogranites and Li-mica granites on the post-collisional stage.

5. Conclusion

All worldwide known rare occurrences of the Phanerozoic rapakivi relate to only those collisional orogens, which border Precambrian cratons and contain HP-UHP metamorphic terranes suggesting the connection of their origin with a deep subduction of the ancient continental crust. The Jangart rapakivi plutons of the Early Permian age are genetically related to unique mega-melange (mega-breccia) terrane that was probably formed in the course of the late-collisional diapiric style exhumation of a partially molten slice of the previously subducted Tarim platform basement. In this connection large blocks of the Tarim metamorphic basement occurring in the center of the mega-melange terrane deserve to be checked for the presence of UHP minerals, in spite of high possibility that those minerals could be erased by the high-temperature metamorphic overprint during heating and exhumation.

In contrast with their Proterozoic counterparts, which are anorogenic, the Phanerozoic rapakivis have been emplaced mostly in the late-postcollisional tectonic setting. The term “synextensional granite” can be used to a better definition of their tectonic character.

Like some other high-temperature igneous rocks such as komatiite, rapakivi belongs to those remarkable rock “species” that being common in the Precambrian almost came to “extinction” toward the Proterozoic termination owing general cooling of the Earth, but still have “survived” in the Phanerozoic. The study of these relict rocks can gain an important insight into the geological evolution of the Earth.

References

1. Alekseev, D.V. and etc. The age and tectonic setting of volcanic and cherty sequences in the ophiolite complex of the Atbashy Ridge (Southern Tien Shan). *Dokl. Earth Sci.* 413A, 380-383.
2. Anderson, J.L., Bender, E.E., 1989. Nature and origin of Proterozoic A-type granitic magmatism in the southwestern United States. *Lithos* 23, 19-52.
3. Bakirov, A.B., 1978. Tectonic Setting of Metamorphic Units in the Tien Shan. Him Press, Frunze, 261 pp. (in Russian).
4. Bazhenov, M.L. and etc. 1999. Permian paleomagnetism of the Tien Shan fold belt, Central Asia: postcollisional rotation and deformation. *Tectonophysics* 312, 303-329.
5. Biske, Yu S., 1996. Paleozoic Structure and Geologic History of the South Tien Shan. St. Petersburg University Press, 192 pp. (in Russian).
6. Biske, Yu S., Shilov, G.G., 1998. The tectonics of the northern margin of the Tarim platform. *Geotectonics* 2, 51-59 (in Russian).
7. Biske, Yu S. and etc. 2012. Structures of the Late Paleozoic thrust belt in Chinese South Tian Shan. *Doklady Earth Sci.* 442, 74-78.
8. Bohlen, S.R., Boettcher, A.L., 1982. The quartz-coesite transformation: a pressure determination and effect of other components.]. *Geophys. Res.* 87, 7073-7078. Boutelier, D.A., Chemenda, A.I., 2008. Exhumation of UHP/LT rocks due to local reduction of the interplate pressure: thermo-mechanical physical modelling. *Earth Planet. Sci. Lett.* 271, 226-232.
9. Brueckner, H.K., 2009. Subduction of continental crust, the origin of postorogenic granitoids and the evolution of Fennoscandia. *J. Geol. Soc., Lond.* 166, 753-762.
10. Burov, E., Francois, T., Yamato, P., Wolf, S., 2014. Mechanism of continental subduction and exhumation of HP and UHP rocks. *Gondwana Res.* 25, 439-880. Calzia, J.P., Ramo, O.T., 2005. Miocene rapakivi granites in the southern Death Valley region, California, USA. *Earth-Sci. Rev.* 73, 221-243.
11. Chen, C., Lu, H., Jia, D., Cai, D., Wu, S., 1999. Closing history of the Tianshan ocean basin, western China: an oblique collisional orogeny. *Tectonophysics* 302, 23- 40.
12. Chen, Y., Zheng, Y., Hu, Z., 2013. Synexhumational anatexis of ultrahigh-pressure metamorphic rocks: petrological evidence from granitic gneiss in Sulu orogen. *Lithos* 156, 69-96.
13. Christiansen, E.H., Burt, D.M., Sheridan, M.F., Wilson, R.T., 1983. The petrogenesis of topaz rhyolites from the western United States. *Contribut. Mineral. Petrol.* 83, 16-30.
14. Clifta, P.D. and etc. 2004. Rapid tectonic exhumation, detachment faulting and orogenic collapse in the Caledonides of western Ireland. *Tectonophysics* 384, 91-113.
15. Collins, W.J. and etc. Nature and origin of A- type granites with particular reference to southern Australia. *Contribut. Mineral. Petrol.* 80, 189-200.
16. Cottle, J.M. and etc. Structural insights into the early stages of exhumation along an orogeny- scale detachment: the South Tibetan Detachment System, Dzaka Chu section, Eastern Himalaya. *J. Struct. Geol.* 29, 1781-1797.
17. Darnley, A.G., 1986. High heat production (HHP) granites, hydrothermal circulation and ore genesis. *Inst. Min. Metall. Trans.* 95, B46-B50.
18. Davies, G.F., 2011. *Mantle Convection for Geologists*. Cambridge University Press, New York, 230 pp.
19. De Grave, J., Glorie, S., Ryabinin, A., Zhimulev, F., Buslov, M.M., Izmer, A., Elburg, M., Vanhaecke, F., Van den haute, P., 2012. Late Paleozoic and Mezo-Cenozoic tectonic evolution of the southern Kyrgyz Tien Shan: constraints from multi-method thermochronology in the Trans-Alai, Turkestan-Alai, segment and southeast Fergana Basin. *J. Asian Earth Sci.* 44, 149-168.
20. Eby, G.N., 1992. Chemical subdivision of A-type granitoids: petrogenetic and tectonic implication. *Geology* 20, 641-644.
21. Geological map of China, in scale 1: 500000, 1989. <<http://www.zonu.com/detail-en/2011-07-27-14150/Geological-map-of-China-l-1989.html>>.
22. Gordon, S.M., and etc. Multi-stage exhumation of young UHP-HP rocks: timescales of melt crystallization in D'Entecasteaux Islands, Southern Papua New Guinea. *Earth Planet. Sci. Lett.* 351-352, 237-246.
23. Haapala, I., Ramo, O.T., Frindt, S., 2005. Comparison of Proterozoic and Phanerozoic rift-related basaltic-granitic magmatism. *Lithos* 80, 1-32.